ULTRA-SHORT ELECTRON BUNCH AND X-RAY TEMPORAL DIAGNOSTICS WITH AN X-BAND TRANSVERSE DEFLECTING CAVITY*

P. Krejcik†, Y. Ding, J. Frisch, Z. Huang, H. Loos, J. W. Wang, M-H. Wang,
SLAC, Menlo Park, CA, USA
C. Behrens, DESY, Hamburg, Germany
P. J. Emma, LBNL, Berkeley, CA, USA

Abstract

The technique of streaking an electron bunch with a RF deflecting cavity to measure its bunch length is being applied in a new way at the Linac Coherent Light Source with the goal of measuring the femtosecond temporal profile of the FEL photon beam. A powerful X-band deflecting cavity is being installed downstream of the FEL undulator and the streaked electron beam will be observed at an energy spectrometer screen at the beam dump. The single-shot measurements will reveal which time slices of the streaked beam have contributed to the FEL process by virtue of their greater energy loss and energy spread relative to the non-lasing portions of the electron bunch. Since the diagnostic is located downstream of the undulator it can be operated continuously without interrupting the beam to the users. The resolution of the new X-band system will be compared to the existing S-band RF deflecting diagnostic systems at SLAC and consideration is given to the required RF phase stability tolerances required for acceptable beam jitter on the monitor. Simulation studies show that about 1 fs (rms) time resolution is achievable in the LCLS over a wide range of FEL wavelengths and pulse lengths.

INTRODUCTION

X-ray Free Electron Lasers such as the Linac Coherent Light Source (LCLS) can produce very short pulses of a few femtoseconds (10^{-15}s) duration [1]. This makes them a powerful tool for observing ultrafast phenomena, such as molecular dynamics. The challenge for the accelerator community is to measure this pulse duration at the fs level. An even greater challenge is to measure both the photon pulse duration and the electron bunch since the emission process does not result in a one to one correspondence.

The transverse deflecting cavity (TCAV) is now a well established diagnostic instrument at FEL linacs to measure the temporal profile and slice properties of the electron beam [2]. In this new application the instrument is installed downstream of the undulator where it streaks the spent electron beam and is observed on a profile monitor screen located at the beam dump [3]. This gives a unique opportunity to observe the FEL process in the time-resolved energy profile of the beam without interrupting beam to the users.

*This work was supported by Department of Energy Contract No. DE-AC0276SF00515
† Corresponding author email pkr@slac.stanford.edu

EXISTING TCAV SYSTEM AT SLAC

Two transverse deflecting cavities are currently in use on the LCLS accelerator and operate at the S-band, 2856 MHz. A short 40 cm section is located in the injector and a longer 2.44 m long structure is located in the main linac, downstream of the second bunch compressor. Both of these structures were actually designed and built in the 1960's [4]. The principle of operation is shown in Figure 1, where a bunch at 0° phase crossing of the rf appears streaked on a downstream screen.

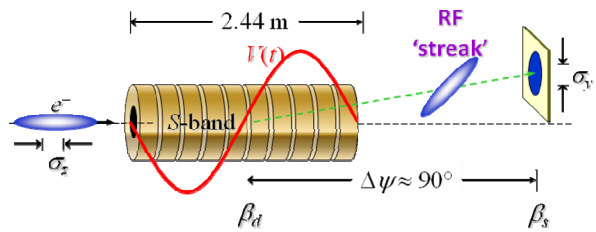

Figure 1: Principle of operation of the TCAV.

The size of the streaked beam σ_y is related to the bunch length σ_z by

$$\sigma_y^2 = \sigma_{y0}^2 + \beta_d \beta_s \sigma_z^2 \left(\frac{k_{RF} e V_0}{E_s} \sin \Delta\psi \cos\phi \right)^2 \quad (1)$$

where σ_{y0} is the unstreaked transverse beam size, β_d and β_s are the beta functions at the deflector and screen, k_{RF} the wave number, V_0 the rf amplitude, E_s the beam energy $\Delta\psi$ the betatron phase advance from deflector to screen and ϕ the phase of the rf.

TCAV Operated with an Energy Spectrometer

The utility of the TCAV diagnostic is further enhanced if the beam is observed on an energy spectrometer screen where the energy dispersion is in the plane perpendicular to the rf deflection. The screen measurement reveals the time-resolved energy and energy spread. The example shown in Figure 2 is from the straight-ahead energy spectrometer screen where the LCLS injector beam is bent in the horizontal plane onto a beam dump. The beam is streaked in the vertical plane so that the curvature of the on-crest rf acceleration of the beam is observed, as well as the "slice" energy spread of the beam. The latter quantity is particularly important for determining the performance of the FEL.

ISBN 978-3-95450-119-9

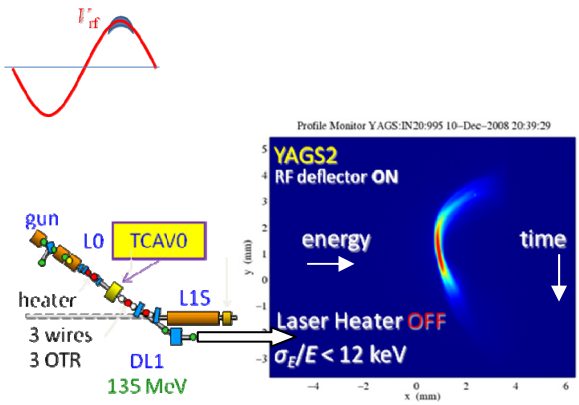

Figure 2: Time-energy correlation measurement.

RESOLUTION OF THE TCAV

The ratio of beam size on the screen to bunch length from Equation (1) is

$$S = \frac{\sigma_y}{\sigma_z} = \frac{k_{rf}\sqrt{\beta_d \beta_s}\,|eV_0 \sin\Delta\psi|}{E_e} \qquad (2)$$

which leads to a measurement resolution in terms of the ratio of the beam emittance $\varepsilon_{N,y}$ to the strength of the kick

$$\sigma_{t,R} = \frac{\sigma_{y0}}{S} = \sqrt{\frac{\varepsilon_{N,y}}{\gamma\beta_d}}\,\frac{\lambda_{rf} E_e}{2\pi |eV_0 \sin\Delta\psi|} \qquad (3)$$

The dependence on wavelength λ_{RF} indicates that we gain a factor 4 in resolution by choosing X-band (λ_{RF}=2.62cm) in place of the existing S-band system ((λ_{RF}=10.5cm). The X-band structure can also be operated at higher field gradients allowing us to achieve a deflection voltage V_0=40 MV which is about 2 times higher than on the existing S-band system. The combined effect is that the new X-band system will have 8 times better resolution. With the typical LCLS beam emittances the expected resolution over the 4-14 GeV beam energy rage is expected to be 1-2 fs.

XTCAV INSTALLATION AT LCLS

Two adjacent 1 m long sections of X-band deflecting structure have been installed at the end of the undulator beamline just before the dumpline dipole bends, as seen in Figure 3. They are fed by a single SLAC XL4 klystron housed together with a modulator in a support building above the undulator tunnel. This is separate from the main linac klystron gallery building and requires a new high-power RF installation and control system. RF waveguide mode converters at the klystron and downstairs at the splitter to the two structures are used to switch between WR90 rectangular waveguide and a low-loss over-moded WC293 circular waveguide for the long run between the klystron and the structures. The XL4 klystron delivers 50 MW peak power at 120 Hz and 40 MW is delivered at the structure input couplers.

Some beamline components have been rearranged to accommodate the XTCAV and optimize the value of the horizontal beta function β_{xd} at the deflector. The new optics is shown in Figure 4.

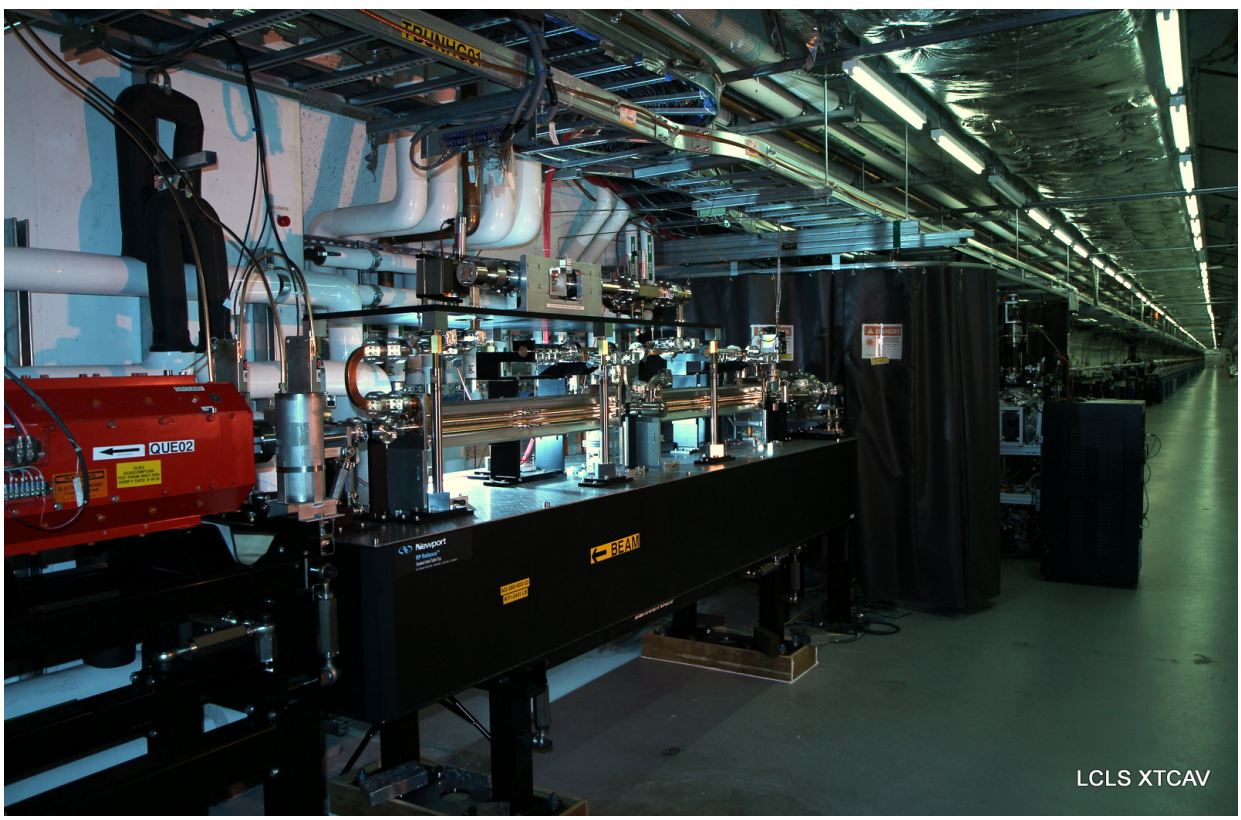

Figure 3: Photo of the XTCAV installed at the downstream end of the undulator beamline.

ISBN 978-3-95450-119-9

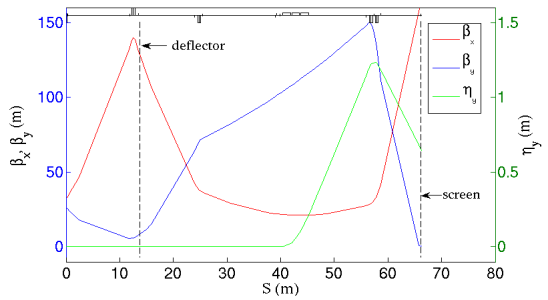

Figure 4: Optics from the deflector to the spectrometer screen.

Operation of the upstream TCAV installations is invasive to user operation of the facility but since the XTCAV is located downstream of the undulator it can be operated continuously with no impact on the FEL. Some precautions are taken with the control system to ensure that accidental mis-phasing of the RF, which results in missteering of the beam, does not unduly trip the Machine Protection System. The parameters for the operation of the XTCAV are summarized in Table 1.

Table 1: Parameters for the XTCAV

Parameter	Value	Unit
RF frequency	11.424	GHz
Structure type	2π/3 backward-wave	
Structure orientation	Horizontal defl.	
Effective structure length	1	m
Total flange-flange length	118.8	cm
Number of structures	2	
No. of regular cells per structure	113	
Aperture 2a	10	mm
Hor. and vert. structure alignment tolerance	< 100	μm
Longitudinal structure positioning tolerance	10	mm
Roll angle tolerance	< 1	mrad
Operating temperature	68	°F
Thermal stability	±0.1	°F
Nominal transverse kick (on crest) @40MW	48	MeV/c
Maximum Repetition rate	120	Hz
RF pulse duration	~ 0.1	μs
RF phase stability (rms) >0.5 Hz	< 0.1	deg-X
RF relative ampl. stability (rms)	1	%
Nominal power required at structure input	40	MW
Max power output from klystron	50	MW

The profile monitor screen where the streaked beam is observed is located immediately in front of the main beam dump where the beam has been bent vertically down to separate it from the photon beam directed straight ahead to the users. The vertical axis of the screen represents the energy coordinate in the beam image with an energy resolving power given by

$$\sigma_{\delta,R} = \frac{\sqrt{\beta_y \varepsilon_{N,y}}}{D_y} \qquad (4)$$

With a vertical dispersion of D_y=0.65 m this gives a resolution of 7 10^{-6}, or 100 keV at 14 GeV.

The camera at this location will be upgraded to give a wider field of view to observe the streaked beam. The image acquisition controls will be upgraded to 120 Hz.

Operational Tolerances

The phase stability requirements of the RF system are defined by the allowable beam position jitter tolerance at the spectrometer screen. The 0.1° rms X-band phase tolerance listed in Table 1 corresponds to a horizontal motion of one sigma of the horizontal beam size. At larger amplitudes of phase jitter the user will observe that progressively more shots will fall outside of the screen viewing angle. The 0.1° phase tolerance puts in turn an 80 ppm voltage stability requirement on the klystron modulator, which is now achievable with new, state-of-the-art technology.

FEL PHOTON MEASUREMENTS

A characteristic of the SASE process in FEL radiation is that not all parts of the electron bunch radiate uniformly. Spikes occur in the temporal domain and grow randomly from shot to shot out of the noise spectrum. The parts of the electron bunch that do contribute to the lasing process suffer a significantly greater energy loss and energy spread increase than the neighbouring non-lasing portions of the bunch. The XTCAV functions as a time-resolved energy spectrometer and reveals which parts of the bunch have lased and what their longitudinal profile is.

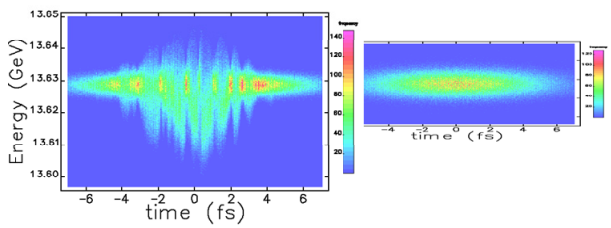

Figure 5: Beam simulation result at the spectrometer screen with the FEL on (left) and FEL off (right).

In the example shown in Figure 5 the electron beam image with the FEL suppressed (at right) is compared to the beam image with the FEL on (left). Lasing in the FEL is easily suppressed by introducing a small steering error in the undulator, taking the electron and photon beam out of coincidence. The portions of the bunch that do lase show up as spikes with an increased energy spread in the vertical plane and a lower centroid energy in the time slice.

Reconstruction of the photon temporal profile

The image is divided horizontally into an arbitrary number of time slices and the centroid energy and energy spread is calculated for each slice. By subtracting the image data taken with the FEL off it is possible to

ISBN 978-3-95450-119-9

quantify the energy shift and energy spread induced by the FEL process itself.

The horizontal projection of the image with the FEL off gives the electron beam current profile before the undulator, as shown in Figure 6 at the left. The beam current profile used in the simulation is the result of start-to-end tracking of the beam, as described in reference [3]. The simulation reflects the complex longitudinal profile of a real beam with higher order terms introduced by compression, CSR and wakefield effects.

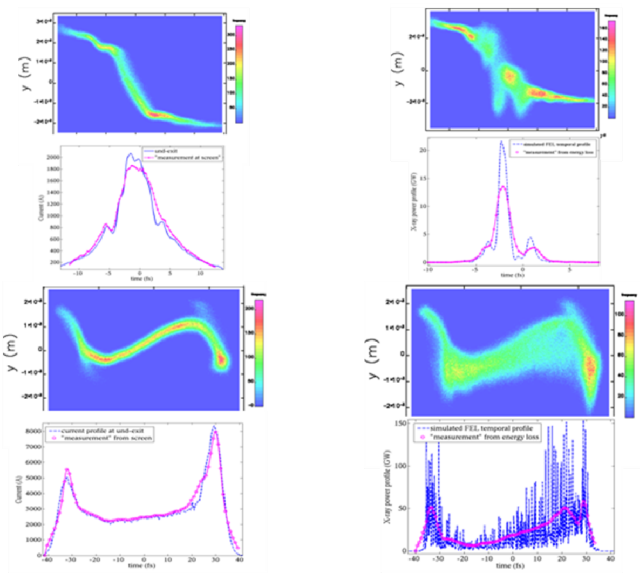

Figure 6: Reconstructed beam current profile (left) and photon intensity (right) for soft x-ray operation (top) and hard x-rays (bottom) from reference [3].

The reconstructed profiles shown on the right in Figure 6 are the predicted photon intensities based on the energy and energy spread inferred from the image. It can be seen that peaks in the laser intensity do no fully coincide with slices of the beam with the highest peak current, further underscoring the need for this diagnostic with its ability to reveal both the electron and photon beam profiles.

ACKNOWLEDGMENT

Grateful acknowledgement is given in memory of the late Ron Akre, who contributed greatly to the many RF projects at SLAC.

REFERENCES

[1] P. Emma et al., Nat. Photon. **4**, 641 (2010).
[2] P. Emma, J. Frisch and P. Krejcik, Report No. LCLS-TN-00-12, 2000.
[3] Y. Ding et al., Phys. Rev. ST Accel. Beams **14**, 120701 (2011).
[4] G. A. Loew and O. H. Altenmueller, "Design and applications of R.F. deflecting structures at SLAC," SLAC-PUB-135, Aug. 1965.

ISBN 978-3-95450-119-9